AD A134 773 NUMERICAL COMPUTATION OF STEADY STATE SCATTERED SOUND EXTERNAL TO SUBMERG..(U) DAVID W TAYLOR NAVAL SHIP RESEARCH AND DEVELOPMENT CENTER BET.. F M HENDERSON 1/1

UNCLASSIFIED OCT 83 DTNSRDC-83/075 F/G 20/1 NL

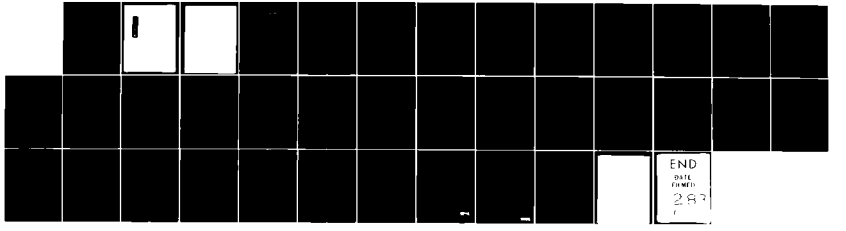

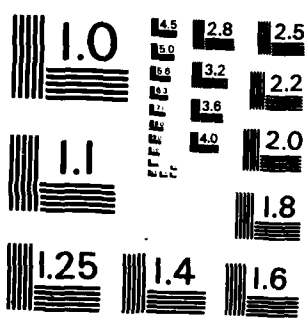

UNCLASSIFIED

SECURITY CLASSIFICATION OF THIS PAGE (When Data Entered)

REPORT DOCUMENTATION PAGE		READ INSTRUCTIONS BEFORE COMPLETING FORM
1. REPORT NUMBER DTNSRDC-83/075	2. GOVT ACCESSION NO. AD-A134773	3. RECIPIENT'S CATALOG NUMBER
4. TITLE (and Subtitle) NUMERICAL COMPUTATION OF STEADY-STATE SCATTERED SOUND EXTERNAL TO SUBMERGED INFINITE CYLINDERS BY COMBINING FINITE ELEMENT AND INTEGRAL EQUATION METHODS		5. TYPE OF REPORT & PERIOD COVERED 6. PERFORMING ORG. REPORT NUMBER
7. AUTHOR(s) Francis M. Henderson		8. CONTRACT OR GRANT NUMBER(s)
9. PERFORMING ORGANIZATION NAME AND ADDRESS David W. Taylor Naval Ship Research and Development Center Bethesda, Maryland 20084		10. PROGRAM ELEMENT, PROJECT, TASK AREA & WORK UNIT NUMBERS (See reverse side)
11. CONTROLLING OFFICE NAME AND ADDRESS		12. REPORT DATE October 1983 13. NUMBER OF PAGES 36
14. MONITORING AGENCY NAME & ADDRESS(if different from Controlling Office) Naval Sea Systems Command (03R11) Washington, D.C. 20360		15. SECURITY CLASS. (of this report) UNCLASSIFIED 15a. DECLASSIFICATION/DOWNGRADING SCHEDULE

16. DISTRIBUTION STATEMENT (of this Report)

APPROVED FOR PUBLIC RELEASE: DISTRIBUTION UNLIMITED

17. DISTRIBUTION STATEMENT (of the abstract entered in Block 20, if different from Report)

18. SUPPLEMENTARY NOTES

19. KEY WORDS (Continue on reverse side if necessary and identify by block number)

Structural Analogies
Symmetric Potential Formulation
Finite Element
Acoustics
Sound Radiation
Sound Scattering
Wave Equation
Wave Absorbing Boundaries
Integral Equations

20. ABSTRACT (Continue on reverse side if necessary and identify by block number)

In a previously reported investigation, scattered sound pressures and velocity distributions on the surfaces of submerged infinite cylinders ensonified by steady-state plane waves were calculated. The numerical method used for these calculations was based on a finite element formulation of the coupled fluid-structure interaction problem and implemented using the NASTRAN

(Continued on reverse side)

DD FORM 1 JAN 73 1473 EDITION OF 1 NOV 65 IS OBSOLETE
S/N 0102-LF-014-6601

UNCLASSIFIED

SECURITY CLASSIFICATION OF THIS PAGE (When Data Entered)

(Block 10)

SR0140301, Task 15321
Work Unit 1808-010

(Block 20 continued)

computer program. In the present investigation, these pressure and velocity data are used as the basis for numerical calculations of the scattered sound pressures generated in the exterior fields of the cylinders. The method consists of replacing an infinite cylinder by a finite cylinder whose external sound field, in three dimensions (3-D), converges to the required two-dimensional (2-D) field as the cylinder length increases. The field pressures are obtained by numerical quadrature of the HELMHOLTZ integral formulation which relates external field pressures to pressures and normal velocities at the structural surface. Calculated 2-D pressure fields, obtained for rigid and elastic cylinders, are in excellent agreement with analytical results.

TABLE OF CONTENTS

LIST OF FIGURES

ABSTRACT

In a previously reported investigation, scattered sound pressures and velocity distributions on the surfaces of submerged infinite cylinders ensonified by steady-state plane waves were calculated. The numerical method used for these calculations was based on a finite element formulation of the coupled fluid-structure interaction problem and implemented using the NASTRAN computer program. In the present investigation, these pressure and velocity data are used as the basis for numerical calculations of the scattered sound pressures generated in the exterior fields of the cylinders. The method consists of replacing an infinite cylinder by a finite cylinder whose external sound field, in three dimensions (3-D), converges to the required two-dimensional (2-D) field as the cylinder length increases. The field pressures are obtained by numerical quadrature of the HELMHOLTZ integral formulation which relates external field pressures to pressures and normal velocities at the structural surface. Calculated 2-D pressure fields, obtained for rigid and elastic cylinders, are in excellent agreement with analytical results.

ADMINISTRATIVE INFORMATION

The work presented here was conducted with funding from the Naval Sea Systems Command (03R11) under Task Area SR0140301, Task 15321, Work Unit 1808-010.

INTRODUCTION

A previously reported investigation demonstrated the use of a structural analog method[1,2,3*] to numerically[1-3] compute the steady-state scattered sound from submerged infinite cylinders ensonified by plane waves. With this approach, which involves the coupling of a finite-element model of the cylindrical shell with a finite-element representation of the exterior and interior fluid (if present within the elastic shell), one obtains acoustic pressure and velocity at the shell-fluid interface, pressure in the interior fluid, and

*A complete listing of references is given on page 29.

exterior field pressures out to the limit of a fictitious wave-absorbing boundary placed a finite distance from the shell surface.

This report supplements previous work of the author by developing and applying a procedure in which the shell-fluid interface pressures and velocities obtained for an infinite cylinder are modified for use as input to a numerical quadrature which extends the computation of exterior pressures to arbitrary distances from the shell surface.

INTEGRAL FORMULATION FOR EXTERIOR PRESSURE-CONTINUOUS AND DISCRETE FORMS

Although the primary purpose of this investigation is to compute 2-D sound pressure fields, the method developed is rooted in the general 3-D problem which is illustrated in Figure 1. A mathematical basis for analyzing this

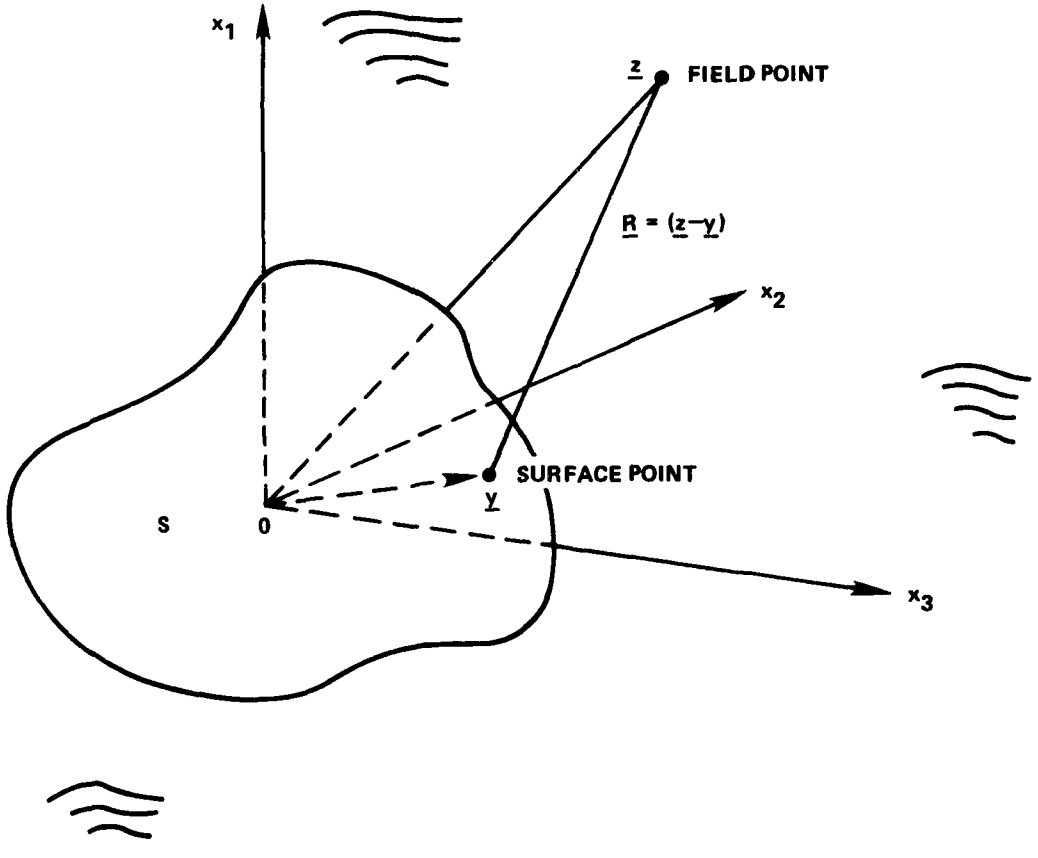

Figure 1 - Geometry of the General Three-Dimensional Exterior Acoustic Field Problem

problem is provided by the Helmholtz integral formulation for the pressure at any arbitrary field point in terms of pressures and normal velocities on an arbitrary closed surface S.

$$\bar{p}(\underline{z}) = -ik \iint_S \bar{v}(\underline{y}) \frac{e^{ik|\underline{z}-\underline{y}|}}{4\pi|\underline{z}-\underline{y}|} dS + \iint_S \bar{p}(\underline{y}) \frac{\partial}{\partial n} \left[\frac{e^{ik|\underline{z}-\underline{y}|}}{4\pi|\underline{z}-\underline{y}|} \right] dS \qquad (1)$$

where $\bar{p}$ = nondimensional pressure $p/\rho c v_o$,

ρ = fluid mass density,

c = speed of sound in the fluid,

v_o = arbitrary velocity,

$\bar{v}$ = nondimensional velocity v/v_o normal to the structural surface,

$\underline{z}$ = vector from coordinate origin to field point,

$\underline{y}$ = vector from coordinate origin to structural surface point,

S = closed surface of the structure,

κ = wave number ω/c, where ω is the angular frequency of the sound waves reflected and/or radiated by the structural surface.

This formulation states that, when a normal velocity distribution $\bar{v}(\underline{y})$ and corresponding pressure distribution $\bar{p}(\underline{y})$ are known for a particular surface, the pressure at a point $\underline{z}$ off the surface can be obtained by a quadrature.

To perform the quadrature, use was made of an algorithm previously coded as part of the XWAVE[4,5] computer program for generalized steady-state radiation and scattering from arbitrarily shaped surfaces. This algorithm follows from a numerical computing method of G. Chertock[6] and is based upon a discretization of the structural surface into a network of patches which need not have uniform density nor any particular uniform shape. One might have, for example, the continuous problem shown in Figure 1, discretized as given in Figure 2. Dots on the surface S denote points that are located at some interior position within each patch. The points within patches are not necessarily at any special positions and need not be uniformly located from one patch to another. These points, with position vectors $\underline{y}_j$ reference discrete stations on the surface where acoustic pressures and normal velocities are assumed known, usually from a previous calculation. The pressure and normal velocity at a station $\underline{y}_j$ are assumed constant over the corresponding patch. The station points also serve as positions for referencing certain geometric

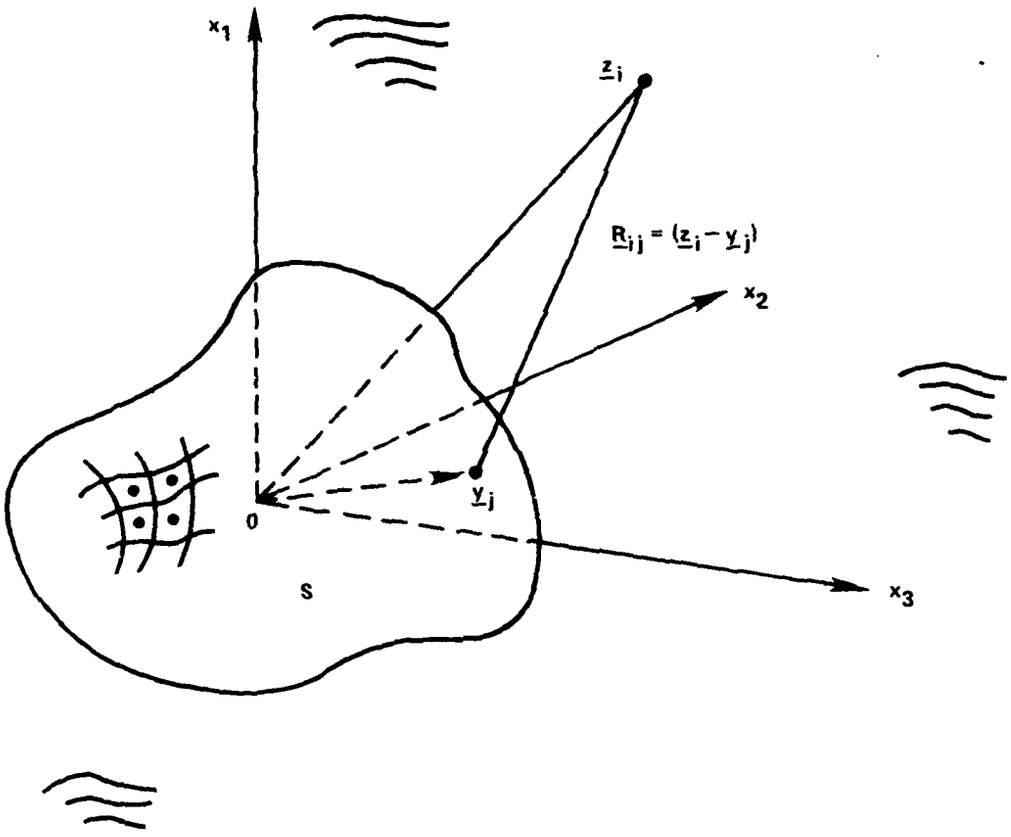

Figure 2 - Discretized Structural Surface for Three-Dimensional Exterior Field Problem

properties of the patch such as area and orientation of unit vectors normal to the surface. With discretization of the structural surface, Equation (1) is replaced by an approximating matrix formulation

$$\{\bar{p}(\underline{z}_i)\} = -ik[\tilde{G}_{ij}][A_{jj}]\{\bar{v}(\underline{y}_j)\} + [\tilde{G2}_{ij}][A_{jj}]\{\bar{p}(\underline{y}_j)\} \qquad (2)$$

for i = 1, 2, ..., M

and J = 1, 2, ..., N

where M = number of field points at which pressure is to be computed

N = number of stations over the structural surface

$\underline{z}_i$ = location of field point

$\underline{y}_j$ = location of a surface station

$[\tilde{G}_{ij}]$ = a matrix of order (M x N) whose coefficients are $e^{ikR_{ij}}/4\pi R_{ij}$, for i = 1, 2, ..., M and j = 1, 2, ..., N

$[\tilde{G2}_{ij}]$ = a matrix of order (M x N) whose coefficients are $\partial/\partial n_j \left[e^{ikR_{ij}}/4\pi R_{ij}\right] \approx e^{ikR_{ij}}/4\pi R_{ij} \left(-ik + 1/R_{ij}\right) \times (\hat{\underline{n}}_j \cdot \hat{\underline{R}}_{ij})$

$\hat{\underline{n}}_j$ = unit outward normal to the structural surface at station j

$\hat{\underline{R}}_{ij}$ = unit vector at station j colinear with $\underline{R}_{ij}$, i.e., $\hat{\underline{R}}_{ij} = \underline{R}_{ij}/R_{ij}$

R_{ij} = $|\underline{R}_{ij}|$

$[A_{jj}]$ = diagonal area matrix whose elements are the patch areas associated with stations j

$\bar{p}(\underline{z}_i)$ = nondimensional acoustic pressure at field point $\underline{z}_i$

$\bar{p}(\underline{y}_j)$ = nondimensional acoustic pressure at surface station $\underline{y}_j$

$\bar{v}(\underline{y}_j)$ = nondimensional normal velocity outward from surface station $\underline{y}_j$

MODIFICATION OF PRESSURES AND VELOCITIES FROM THE STRUCTURAL ANALOG COMPUTATION

The previous section indicates clearly that once a particular surface geometry along with known pressure and normal velocity distributions over this surface have been specified, the numerical quadrature for exterior field pressures is straightforwardly obtained given sufficient computer memory and running time which may be required in applications involving very large numbers of surface patches. No matrices need be inverted nor integrand singularities considered. Care need only be taken to ensure that the pressure and velocity data, which are input to the quadrature algorithm, are (1) consistent with the formulation on which the quadrature is based and (2) consistent with respect to the field pressure being computed.

Attention to condition (1) is especially warranted in instances where computing methods of somewhat diverse origin are being interfaced to achieve the field calculation. For example, in this investigation a finite-element approach is to be interfaced with a method (the quadrature algorithm) whose formulation is derived from the area of acoustic analysis. It so happens that sign conventions used in the exponential factor for time dependence are different in the particular programs being coupled: in NASTRAN (the structural analysis program) the convention is $e^{i\omega t}$, whereas in XWAVE (the acoustics program) it is $e^{-i\omega t}$. As a result, the first and most basic modification required for pressures and velocities in complex form (a+bi), generated by the analog computation, is conjugation to the form (a-bi).

Whether or not the conjugated data require further modification to satisfy condition (2) depends partially upon the type of scattering being computed and partially on the philosophy adopted for managing data input to the finite element and quadrature computations. Some specific examples from rigid and elastic scattering will illustrate. In these examples it will be assumed that the field quantity to be directly computed is the scattered (as opposed to total) pressure.

RIGID SCATTERING

Figure 3 shows a perspective view of a portion of the inner boundary of the finite element model for fluid exterior to a rigid cylinder.[1] The fluid is modeled with quadrilateral membrane elements of an arbitrarily chosen thickness of 1 meter, (since the cylinder is infinite). Since the finite-element formulation of steady-state rigid scattering is based upon a velocity potential form of the wave equation, the prescribed boundary condition at the structural surface is

$$-\frac{\partial \phi}{\partial n} = v_n \qquad (3)$$

where v_n is the normal component of the scattered particle velocity directed into the exterior field of the cylinder. For rigid scattering, v_n is a known quantity, depending only upon the magnitude, frequency, and direction of the incident wave and the geometry of the structural surface.

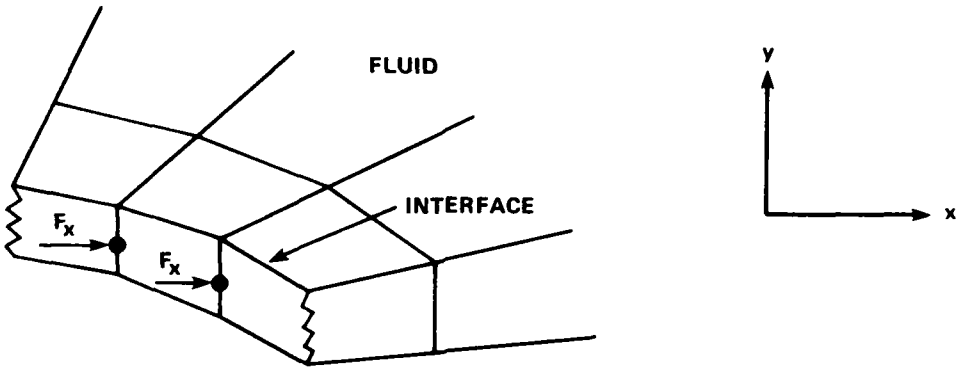

Figure 3 - Finite-Element Model of Fluid-Structure Interface for Rigid-Scattering

The structural analog of v_n for the finite-element model is a set of forces acting at grid points on the inner boundary of the fluid model as given in Figure 3. The relationship between these forces and the normal velocity is (see Equation (6) of Reference 1),

$$-F_x = \mu_e A v_n \tag{4}$$

where μ_e is the shear modulus assigned to the fluid finite elements, the e denoting a generally nonstandard value for μ, and A is the area associated with a grid point. With a set of input, $-F_x$, one then obtains from the finite-element computation the corresponding rigid scattered pressures, $p_{s\omega}$, on the cylinder. The computed pressures with the corresponding normal velocity distribution, v_n, is a consistent set of boundary data for input to the field calculation when both pressure and velocity are conjugated.

Although the v_n can be computed analytically, it is perhaps more convenient to extract them from the NASTRAN data input to the finite-element computation. As a basis for this, expand Equation (4) as follows,

$$-F_x = \mu_e A v_n = \mu_e A V(x) \cos\theta e^{-i\omega\tau} \tag{5}$$

where $V(x)$ = magnitude of particle velocity in an incident plane wave with frequency ω.

θ = projection angle, Figure 4, for obtaining a component of $V(x)$ normal to the cylinder surface and pointing into the fluid.

τ = time delay for incident wave passage from P_1 to P_2, see Figure 4.

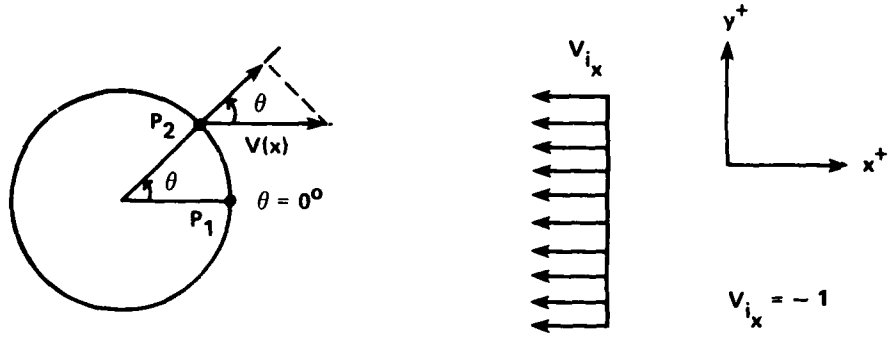

Figure 4 - Geometry Relating to the Computation of the Structural Surface Normal Component of Incident Velocity

Since the incident wave particle velocity is assumed to have unit magnitude, Equation (5) becomes

$$-F_x = \mu_e A \cos\theta \, e^{-i\omega\tau} \tag{6}$$

Since NASTRAN's facility for specifying frequency-dependent loads was used to input the loads F_x for the computations, DAREA data cards were used to enter the quantity $\mu_e A \cos\theta$ for each fluid grid point on the cylindrical surface. Also available in the input data are the x-coordinates of these grid points. Using these coordinates and the cylinder radius, r, one obtains

$$\cos\theta = x/r \tag{7}$$

for each of the grid points. From Equation (5), the surface normal velocity is then obtained as

$$V_n = \frac{-F_x}{\mu_e A \cos\theta} \times \cos\theta = \frac{-F_x}{\mu_e A} \tag{8}$$

which becomes

$$v_n = -F_x/A \tag{9}$$

with substitution of $\mu_e = 1$ in accordance with the analog formulation for rigid scattering.

If just the absolute value of the exterior field pressure is of interest, one can as a second option, specify equally well the negative of F_x in Equation (6), by assigning to μ_e the value -1, which is also required for reasons of symmetry in the elastic scattering case. Since, in vector form, F_x is the complete right-hand side of a matrix equation for displacement, i.e., the analog[1] of the velocity potential, the change in sign of F_x results in a corresponding change in sign for computed pressures. Some care is needed, however, in extracting the corresponding surface normal velocities for use with these pressures in the field calculation. This is so because a routine application of Equation (8) will yield, in this case,

$$\frac{F_x}{-A\cos\theta} \times \cos\theta = \frac{-F_x}{A} = v_n \tag{10}$$

whereas the normal velocity corresponding to negative scattered pressure, $-p_{s\infty}$ is $-V_n$. This clearly indicates that to obtain normal velocities consistent with the computed pressures, $-p_{s\infty}$, in this case, one must negate the normal velocities extracted in the above manner from the input data. This modification is in addition to the requirement for conjugation of both quantities as previously discussed. The use of negative normal velocity distributions in computing structural surface pressures will be shown later to offer

advantages in the handling of data input to the finite-element computations when both rigid and elastic scattering are being computed for the same structure.

ELASTIC SCATTERING

For the case of elastic scattering, the cylindrical shell actively interacts with the fluid and is explicitly modeled along with the fluid; the symmetric velocity potential method is used to symmetrize the structure-fluid interaction equations in matrix form.[1,2,3] Because the fundamental fluid unknown is the integral of pressure,[1,2,3] fluid pressure can be recovered from the finite-element program by listing the first derivatives (velocity of the unknown).

As in the previous case, the conjugate of the computed pressure at the cylinder surface gives one set of boundary data required for the field calculation. This pressure is symbolized by p_{se} which denotes pressure scattered by an elastic boundary. The corresponding surface normal velocity will be designated $V_{n_{se}}$. To see how $V_{n_{se}}$ can be obtained, it is convenient to begin with an expression[7] for p_{se} in terms of its components,[7]

$$p_{se} = p_{s\infty} + p_r \tag{11}$$

where $p_{s\infty}$ is the pressure scattered by a rigid structural surface and p_r is the pressure radiated by elastic motion of the structural surface. At the surface of the structure one can write

$$\frac{\partial p_{se}}{\partial n} = \frac{\partial p_{s\infty}}{\partial n} + \frac{\partial p_r}{\partial n} \tag{12}$$

where n denotes the direction normal to the surface and into the exterior fluid. Substituting in Equation (12) the boundary condition satisfied by each term,

$$\begin{aligned} \frac{\partial p_{se}}{\partial n} &= -\rho \ddot{w}_{se} \\ \frac{\partial p_{s\infty}}{\partial n} &= -\rho \ddot{w}_{s\infty} \\ \frac{\partial p_{r}}{\partial n} &= -\rho \ddot{w}_{r} \end{aligned} \tag{13}$$

where w is the surface normal displacement of fluid particles adjacent to the boundary surface and the dots denote the time differentiation, and dividing by $-\rho$, gives

$$\ddot{w}_{se} = \ddot{w}_{s\infty} + \ddot{w}_{r} \tag{14}$$

Integrating Equation (14) once and letting $v = \dot{w}$, gives

$$v_{n_{se}} = v_{n_{s\infty}} + v_{n_{r}} \tag{15}$$

The first term on the right-hand side of Equation (15) is simply the normal surface velocity which appeared in the boundary condition, Equation (3), for rigid scattering. The second term is the radial velocity of the shell obtained directly from the structural analog computation. As an interesting sidelight, it may be noted that this velocity, which is the in-fluid velocity of the shell, can be obtained analytically (Equations (12.31) and (12.32) in Reference 7) for infinite, thin cylindrical shells. As part of this investigation, the analytic expressions were coded for numerical evaluation. The analytic values for v_{n_r} were in good agreement with the finite element results.

Equation (15) then indicates that the shell boundary velocity required for the field pressure calculation is obtained by adding the rigidly scattered normal surface velocity, an input quantity for the finite-element calculation, to the in-fluid radial shell velocity, an output quantity from that calculation. As in the case for the rigid scattering analog calculations, $v_{n_{s\infty}}$ is

input via frequency-dependent loads F_x, for Equation (6). In the elastic case, however, the sign of μ_e must be negative. This condition results from the fact that the symmetric potential formulation involves multiplication of the equations in one partition of the matrix formulation for the elastic structural analog by $-1/\rho$. This multiplication is achieved for matrix coefficients from the left-hand side of the analog equations by specifying a negative shear modulus on the NASTRAN material properties (MAT1) data card. The negative sign of μ_e in F_x takes care of the corresponding multiplication for terms on the right-hand side of the equations. Since μ_e, as pertaining to F_x, is incorporated in data on the DAREA cards, the DAREA quantities will be $-A\cos\theta$, and hence, $v_{n_{s\infty}}$ can be readily extracted from the F_x loads as in Equation (10). Adding this velocity to v_{n_r} and conjugating the result yields the velocity distribution consistent with p_{se} for the field calculation.

The requirement for a negative μ_e in specifying F_x emphasizes the convenience of the second option discussed, on page 9 , for specifying F_x in the rigid scattering case (Equation (6)), namely, that it allows DAREA data for rigid calculations to be carried over to elastic calculations or vice versa.

ADAPTATION OF THREE-DIMENSIONAL QUADRATURE ALGORITHM TO CALCULATION OF TWO-DIMENSIONAL SOUND FIELDS

Having seen (in the previous section) how to obtain, from the 2-D structural analog calculations, sets of shell surface pressures and velocities which are consistent with the field pressure algorithm as well as each other, consideration is now given to a method of using these data to calculate 2-D sound fields.

The overall strategy of the method is to calculate, as an approximation to 2-D sound fields, the fields of finite cylinders of sufficient lengths that scattering from the ends does not contribute significantly to the field results.

Consider first the acoustic modeling (see Figure 2) of a general finite cylindrical surface which is scattering a plane wave train with the direction of incidence normal to the cylinder's longitudinal axis. Clearly, from the symmetry inherent in this problem, only one quarter of the surface need be modeled; see Figure 5. Ordinarily, for the case of finite cylinders, the end

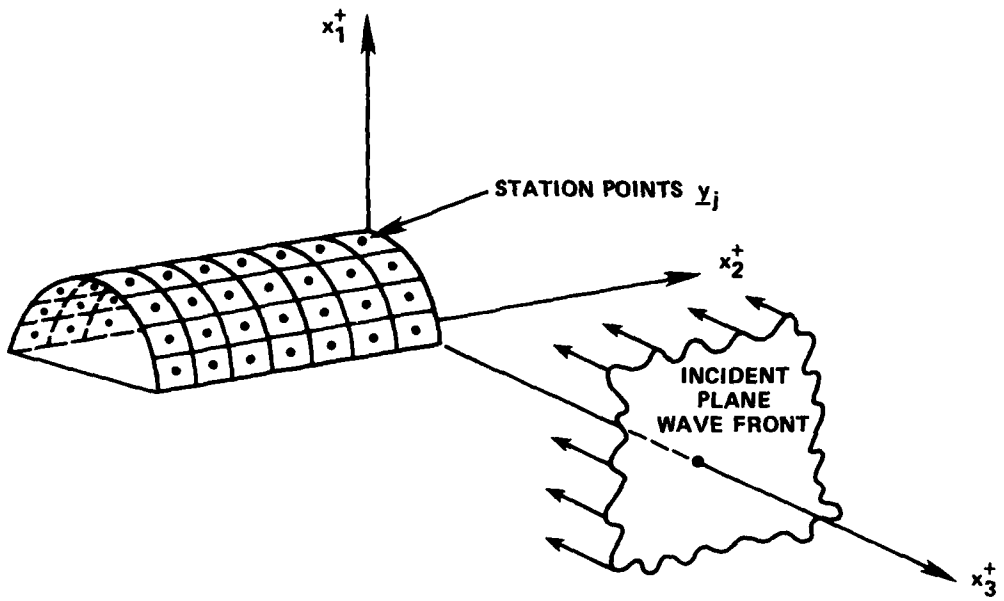

Figure 5 - Surface Acoustic Model for a Finite Cylinder
Scattering an Incident Plane Wave Normal
to the Longitudinal Axis

cap in Figure 5 would also be modeled, but since the length will ultimately negate the end effect, this modeling is omitted from the start. The station points $\underline{y}_j$ (see Figure 2) are located at the midpoints of the acoustic elements or patches of surface area. In interfacing the finite element and acoustics program, the station points can be made to coincide with grid points of the finite element model.

Although the integral formulation for field pressure offers considerable generality of application as previously discussed (pages 2-5), it can be shown to be greatly simplified in the present case if the field pressure is calculated at points along the x_3 axis of the cylinder's coordinate system; see Figure 6. It is seen that, as a result of structural surface symmetry, each acoustic element on the quarter surface modeled has three reflected image

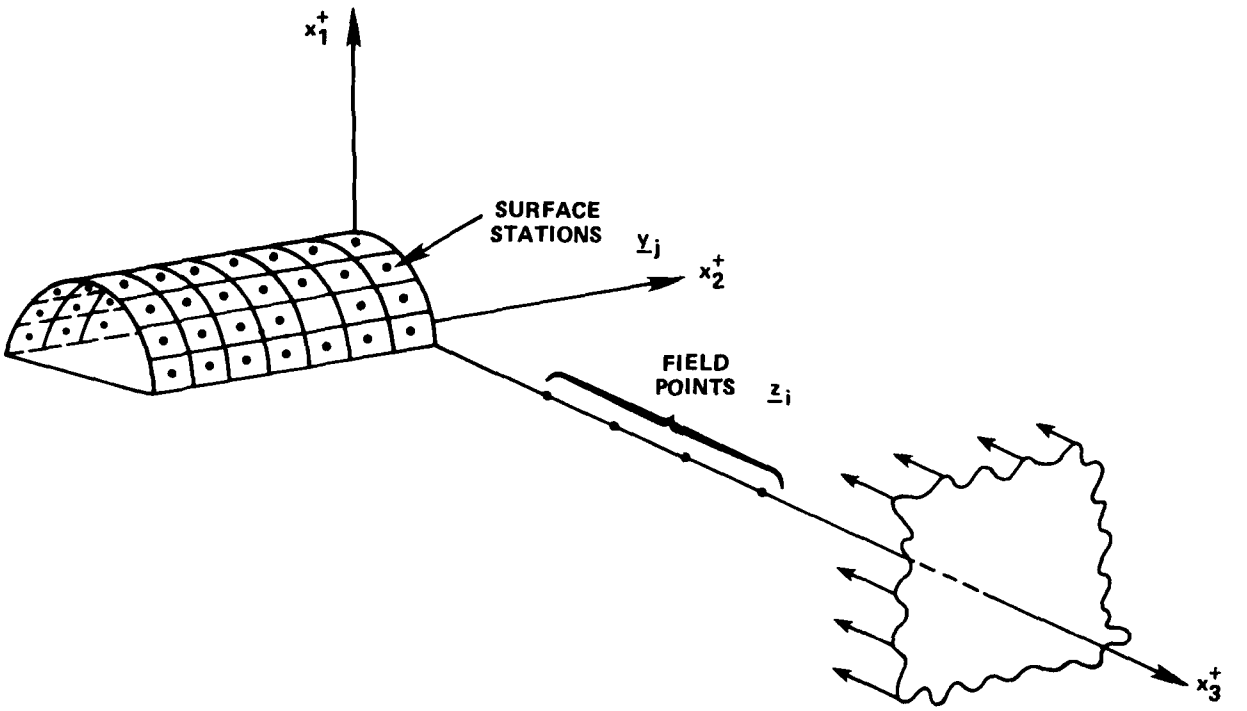

Figure 6 - Geometry for Field Pressure Calculations

elements in the coordinate planes. If an element is identified with its station point, this reflection can be expressed,

$$\underline{y}_j \xrightarrow{x_2x_3} \underline{y}'_j \xrightarrow{x_1x_3} \underline{y}''_j \xrightarrow{x_2x_3} \underline{y}'''_j \xrightarrow{x_1x_3} \underline{v}_j \qquad (16)$$

where the symbol $\xrightarrow{x_n x_m}$ denotes reflection in the plane defined by coordinates x_n and x_m. The pressure at a general field point $\underline{z}_i$ due to an acoustic element

j and its image elements is, from Equation (2)

$$\bar{p}_i = -ik(\tilde{G}_{ij}A_j\bar{v}_j + \tilde{G}_{ij}'A_j'\bar{v}_j' + \tilde{G}_{ij}''A_j''\bar{v}_j'' + \tilde{G}_{ij}'''A_j'''\bar{v}_j''') + (\tilde{G2}_{ij}A_j\bar{p}_j + \tilde{G2}_{ij}'A_j'\bar{p}_j' + \tilde{G2}_{ij}''A_j''\bar{p}_j'' + \tilde{G2}_{ij}'''A_j'''\bar{p}_j''') \quad (17)$$

It can be readily shown that if a field point i on x_3 is paired with surface element j or any of its images in the coordinate planes, the formula for the corresponding coefficients $\tilde{G}$ (page 5) yields quantities of the same magnitude and sign, and similarly for the quantities $\tilde{G2}$. Since the velocity $\bar{v}$ is the same for surface element j and its images, the pressure will likewise be the same, and Equation (17) can be reduced to

$$\bar{p}_i = 4(-ik\tilde{G}_{ij}A_j\bar{v}_j + \tilde{G2}_{ij}A_j\bar{p}_j) \quad (18)$$

The pressure at i due to the entire cylinder, less end caps, is then given by

$$\bar{p}_i = 4\sum_{j=1}^{N}(-ik\tilde{G}_{ij}A_j\bar{v}_j + \tilde{G2}_{ij}A_j\bar{p}_j) \quad (19)$$

for j = 1, 2, ... , N where N equals a number of surface elements in the quarter-cylinder; see Figure 6.

As a basis for adapting the integral formulation to 2-D sound calculations, let the surface in Figure 6 be the quarter-portion of the truncation of an infinite cylinder extending from $-\infty$ to $+\infty$ on the x_2 axis. Assume the surface is modeled by consecutive circumferential bands of m elements; see Figure 7. From Equation (19), the pressure at field point $\underline{z}_i$ due to the truncated infinite cylinder is

$$\bar{p}_i = 4\left\{\sum_{j=1}^{m}(-ik\tilde{G}_{ij}A_j\bar{v}_j + \tilde{G2}_{ij}A_j\bar{p}_j) + \sum_{j=m+1}^{2m}(-ik\tilde{G}_{ij}A_j\bar{v}_j + \tilde{G2}_{ij}A_j\bar{p}_j) + \ldots + \sum_{j=(k-1)m+1}^{km}(-ik\tilde{G}_{ij}A_j\bar{v}_j + \tilde{G2}_{ij}A_j\bar{p}_j)\right\} \quad (20)$$

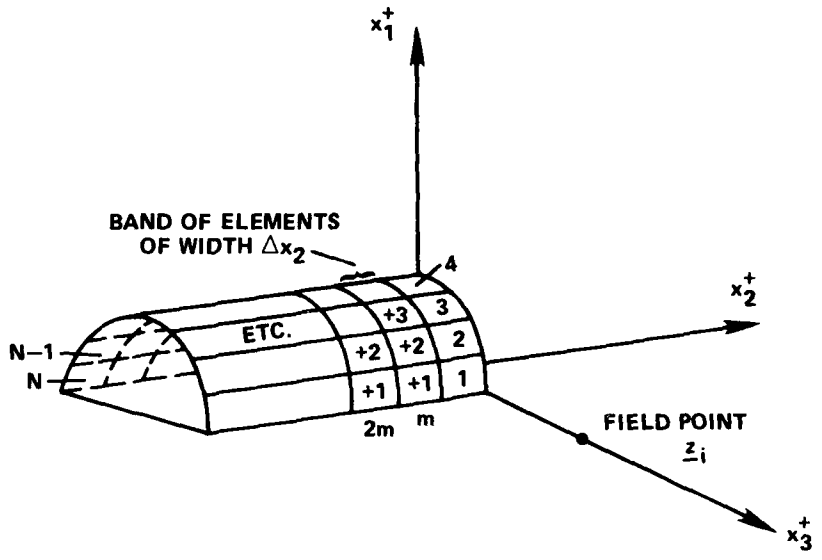

Figure 7 - Numbering of Structural Surface Acoustic Elements

where k is the number of bands. This expression abbreviates to

$$\bar{p}_i = 4(S_1 + S_2 + \ldots + S_k) \tag{21}$$

The strategy for applying the 3-D algorithm to the 2-D sound calculation is to compute and cumulatively add the partial sums S_ℓ until an S_k is reached whose contribution to the total sum, thus far obtained, can be assumed negligible according to some predetermined criterion for stopping the integration. It should be noted that the selection of a robust criterion is not, in general, a trivial matter.[8] Equation (21), in this case, states that the scattered sound field at $\underline{z}_i$, due to a finite cylinder of total length $2k\Delta x_2$, reasonably approximates that of an infinite cylinder.

The last item to be considered in this section concerns the interfacing of the structural surface acoustic model with the surface pressure and velocity data from the finite-element computations. These computations,[1] which are based on a truly 2-D theory, give the pressure and velocity data at grid points which lie on a circular arc in the x_1x_3 plane; see Figure 8. The pressure and velocity at a grid point are constant along a longitudinal line through the

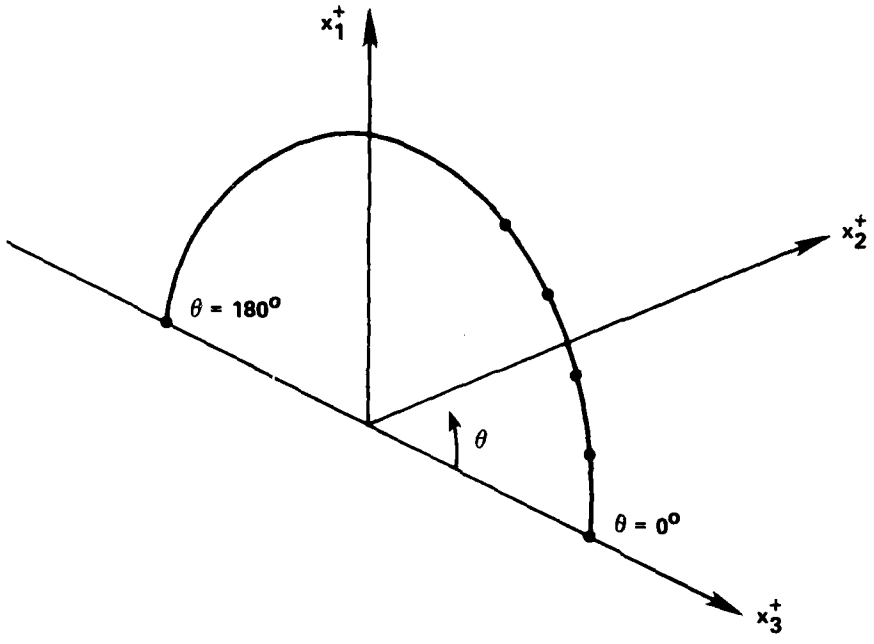

Figure 8 - Grid Point Configuration from Structural Analog Calculations

grid point extending from $-\infty$ to $+\infty$. This configuration immediately suggests two possibilities for interfacing the acoustic model; see Figure 9. In these sketches, dots signify grid points to which pressures and velocities are referenced in the analog calculations. Circles signify, in general, surface points along longitudinal lines of constant pressure and velocity to which the calculated quantities are projected.

It is seen in Figures 9a and 9b, by comparing the two surface models, that the primary difference between them is the way in which computed pressure and velocity at $x_2 = 0$, and $\theta = 0$ are utilized, since this determines whether or not elements in the first circumferential band and elements along the longitudinal line $x_3 = \pm$ radius overlap the respective symmetry planes x_1-x_3, and x_2-x_3. In the first model, Figure 9a, a single acoustic element is centered on the grid point $\theta = 0$, and $x_2 = 0$. The computed pressure and velocity at the grid point are assumed to be constant over the element. In the angular direction, the element extends from $\theta = 0$ degrees to $\pm$ ½ the arc distance from $\theta = 0$

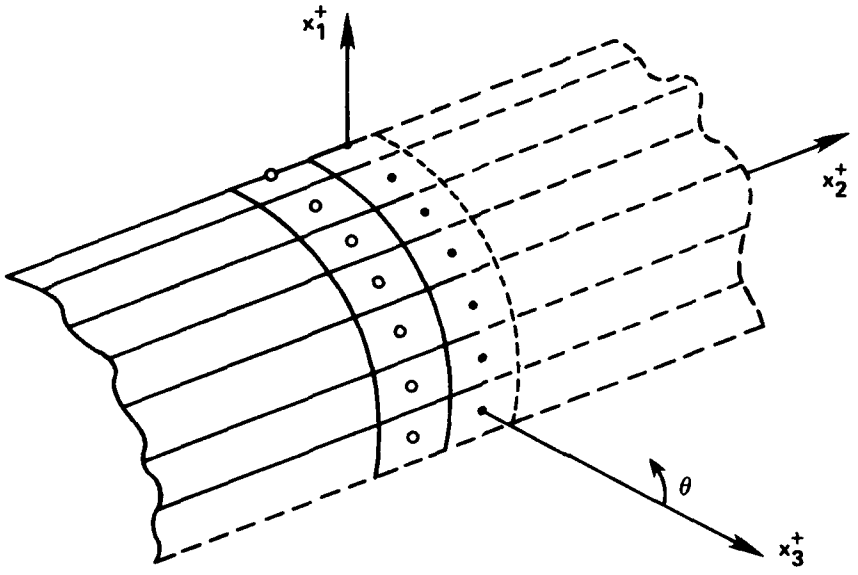

Figure 9a - Acoustic Model Overlapping Two of the Principal Symmetry Planes, $x_1 - x_3$ and $x_2 - x_3$, of the Infinite Cylinder

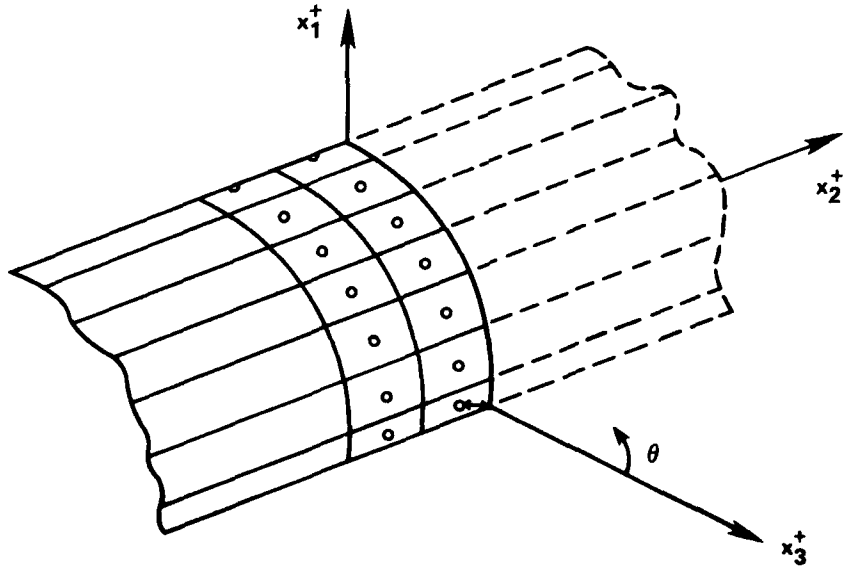

Figure 9b - Acoustic Model Entirely Within the Two Principal Symmetry Planes, $x_1 - x_3$ and $x_2 - x_3$, of the Infinite Cylinder

Figure 9 - Interfacing of the Surface Acoustic Model and Structural Analog Data for an Infinite Cylinder

degrees to the next circumferential grid point. In the longitudinal direction, the element extends from $x_2 = 0$ to $\pm$ ½ the bandwidth (arbitrary within limits, in the case of 2-D) selected for the particular modeling. To obtain the second model, Figure 9b, the pressure and velocity are assumed constant over an element again centered at $\theta = 0$, and $x_2 = 0$ and having the same extent in angular direction, but extending from $x_2 = 0$ to $\pm$ twice the bandwidth selected for the acoustic model. A quarter portion (quadrant) of this element is taken as the first element in the first band of the model with the computed pressure at $\theta = 0$, and $x_2 = 0$, assumed at its midpoint as indicated by arrows $\longleftrightarrow$ in the sketch. Although orientation of the unit normal vector at the midpoint of this element differs from that of its parent, the difference becomes negligible as the structural finite-element grid (as shown in Figure 8) and hence the acoustic surface model is refined for calculations at higher frequencies.

Whereas the first acoustic model, Figure 9a, interfaces more naturally with the structural grid points, the second model, Figure 9b, allows a more uniform handling of symmetries for the field calculation. In particular, it can be seen from Figure 9a that, with respect to surface stations having the same scattered pressure and velocity, the two stations $\theta = 0$ degrees and 180 degrees and $x_2 = 0$ have no reflected images in the principal symmetry planes; the stations $\theta = 0$ degrees and 180 degrees, with $x_2 < 0$ each have one image and all other stations explicitly modeled have three images. This is contrasted with the model in Figure 9b in which every element has three images. Early test calculations using both models gave essentially the same results for field pressures. For this reason and due to less of a need for bookkeeping to keep track of symmetries, Figure 9b became the model of choice for later calculations.

All geometric data (pages 3-4) required for the surface acoustic models were obtained through the use of that portion of XWAVE's[2] automatic data generator which handles cylindrical surfaces. The strategy for core storage of these data differs, however, from that used with finite surfaces having predefined dimensions, in that at any time during the field calculation only the data pertaining to a single band of elements (see Figure 7) resides in storage. After completing the calculation of the band's contribution, S_ℓ to the summation in Equation (21), the current geometric data are updated to that of

the next band $\ell + 1$ in the $-x_2$ direction (see Figure 7). Then the contribution, $S_{\ell+1}$, is computed and the process is continued until the total field calculation is terminated.

CALCULATIONS

Field calculations were made for all distributions of the structural surface normal velocities and pressures obtained from the structural analog results, computed previously, except for the cases at 150 Hz rigid condition and 225 Hz for elastic scattering. Figure 10 is a summary of the physical problem upon which the calculations are based.

The accumulation of partial sums, Equation (21), was carried out until the approximation for the field pressure had converged to the number of significant figures that could be plotted effectively. This condition occurred when the cylinder had grown to approximately the length 2L (~ 655 m). The results thus obtained (see Figure 11-14) are seen to be in very good agreement with those obtained from analytic formulations[7] for rigid and elastic 2-D scattering. These formulations have been implemented by the author for automatic calculation in two special-purpose programs, SCAT1 (rigid) and SCAT2 (elastic). Calculations were made for field points ranging from 1.12 m to 100 m (= 100 diameters) from the cylinder surface.

The field calculation for 225 Hz rigid scattering was found to be essentially insensitive to the accuracy of input surface pressures; recall that the surface normal velocity is analytically obtained in this case. Figure 11 shows, in fact, that the difference between computed and analytic field pressures cannot be plotted anywhere within the range of the distance considered, whereas the error in the surface pressure from the analog calculation is nearly all confined to the illuminated portion of the cylinder (see Figure 12 of Reference 1).

The field calculations for elastic scattering were found to correlate well with the accuracy of input pressures on the illumined surface of the cylinder. It is seen, in comparing Figures 12, 13, and 14, that the largest errors in field pressure occurred for the 2100 Hz case. This would appear to correspond to the fact that, among the finite-element calculations for the frequencies 2100 Hz, 4100 Hz, and 6600 Hz, the one for 2100 Hz yielded the least accurate surface pressures in the neighborhood of $\theta = 0$ degrees (see Figures 19, 22,

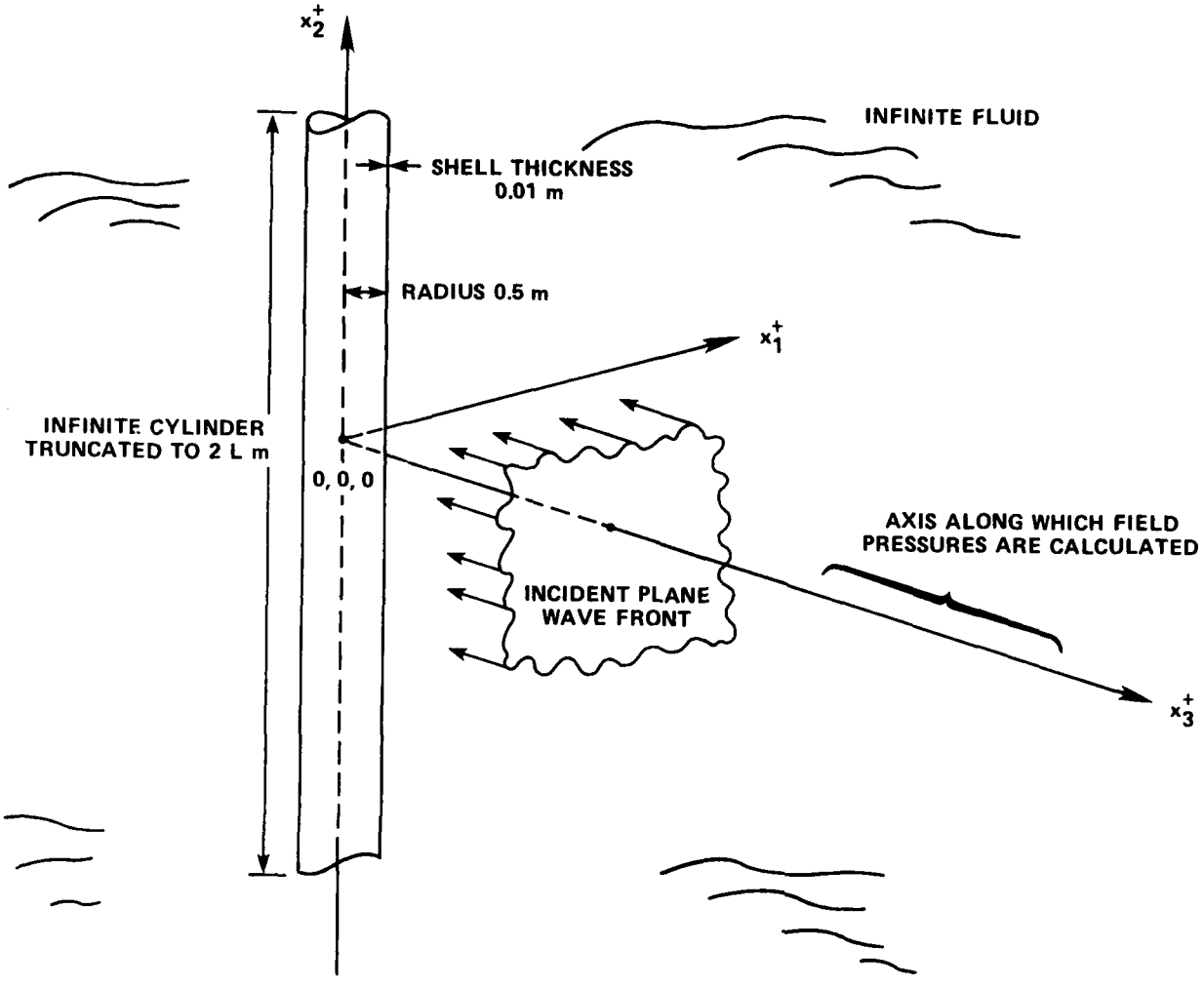

Figure 10 - Sketch of the Physical Problem

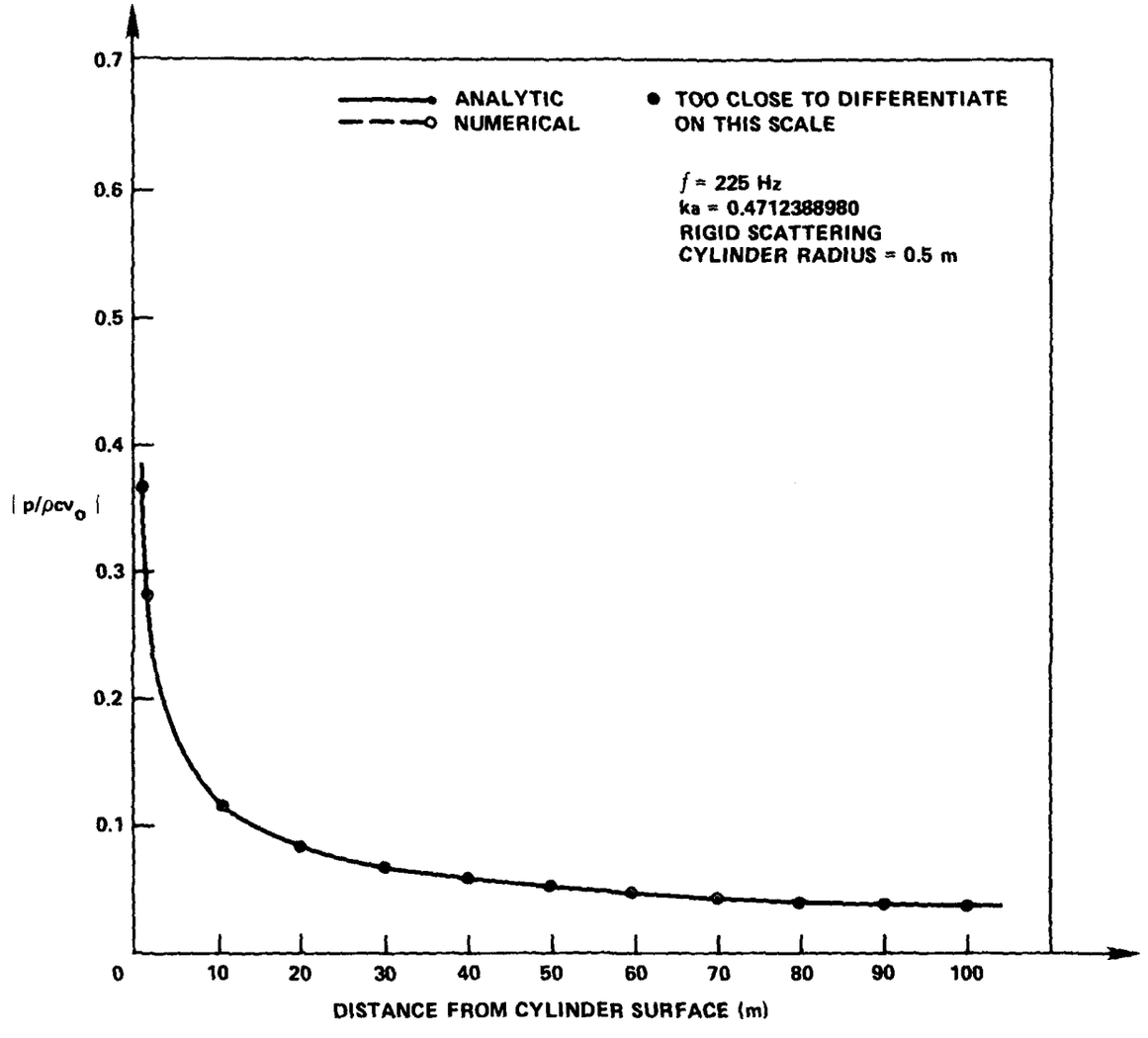

Figure 11 - Field Pressures Calculated for 225 Hertz Rigid Scattering

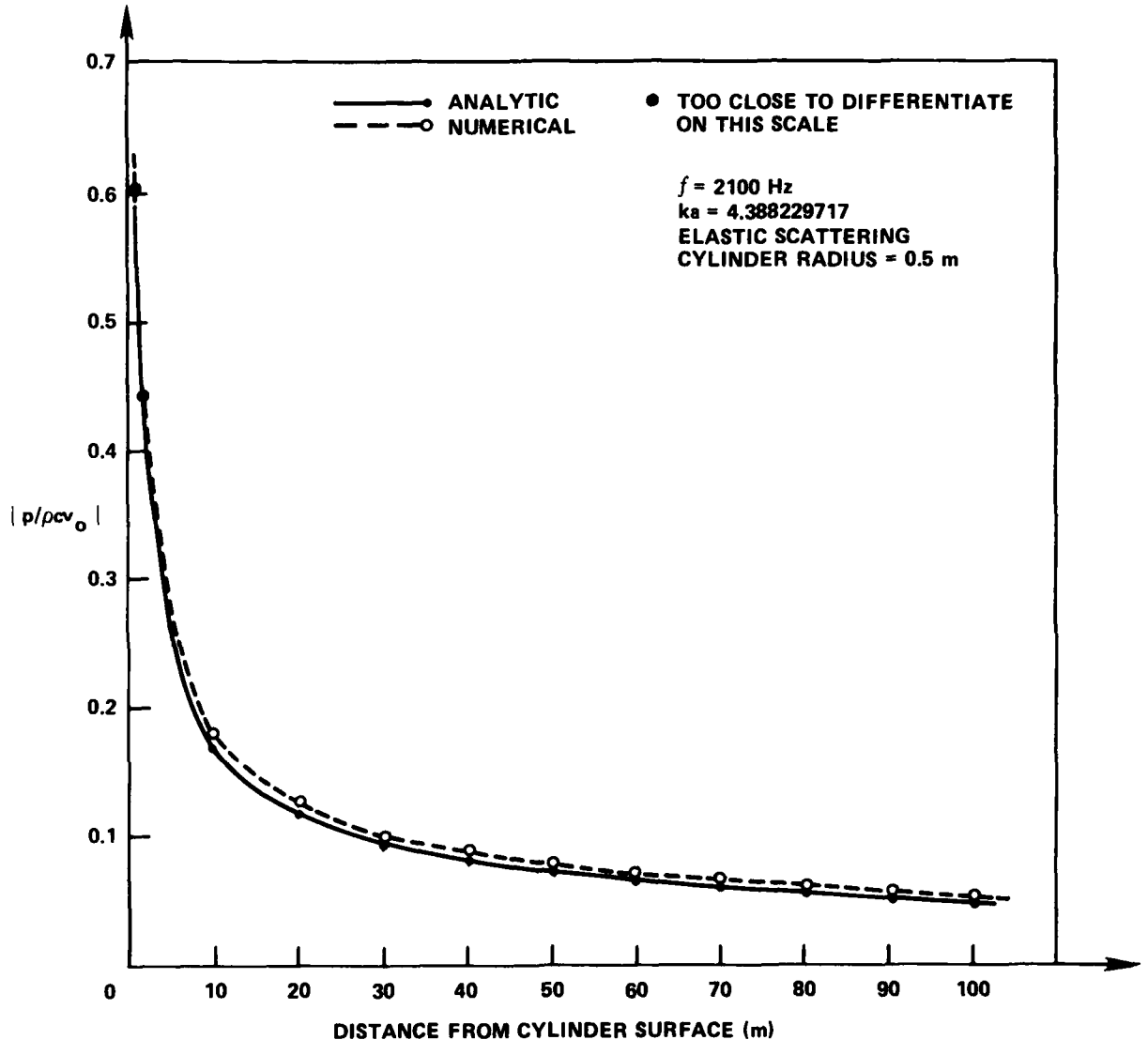

Figure 12 - Field Pressures Calculated for 2100 Hertz Elastic Scattering

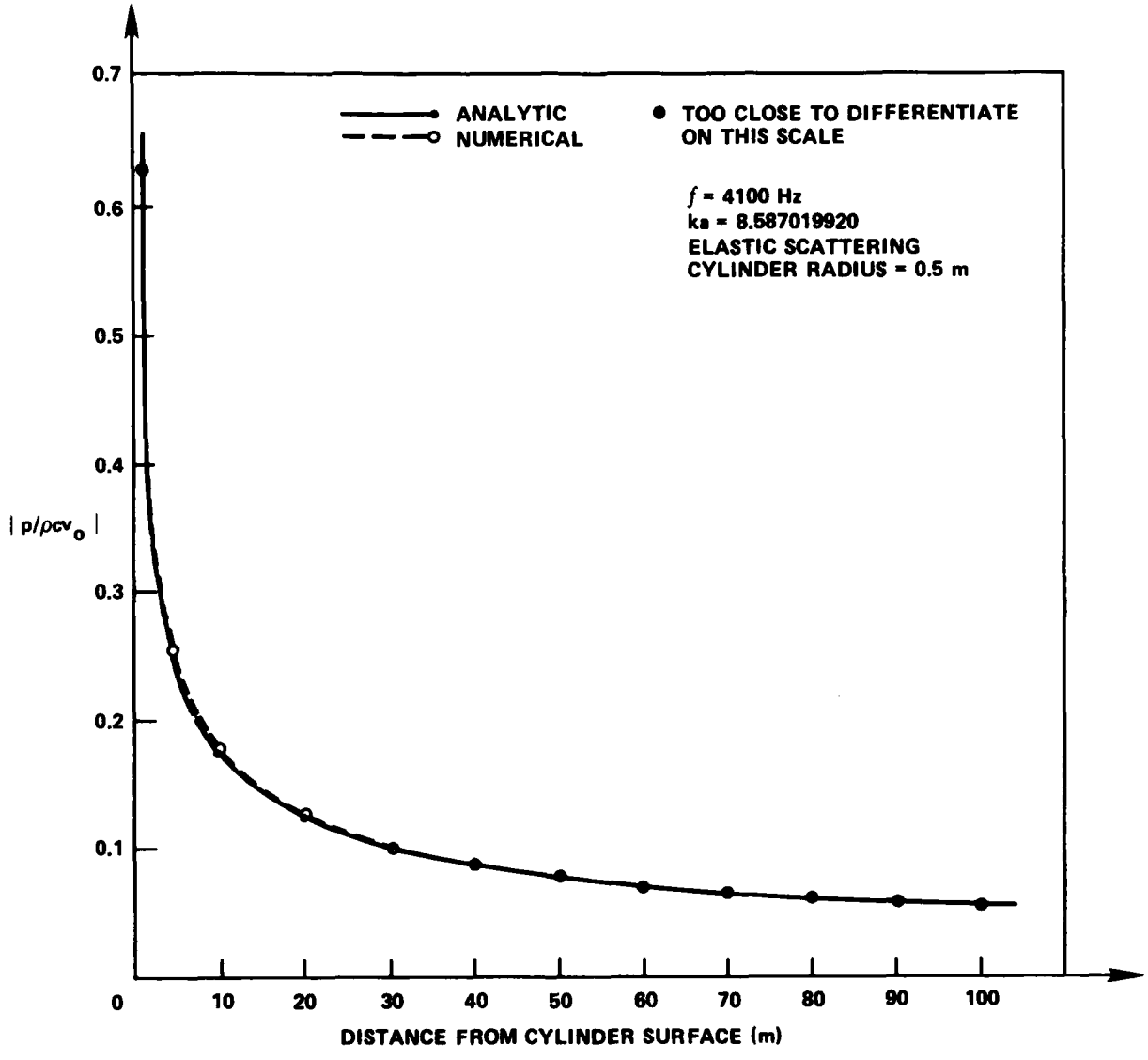

Figure 13 - Field Pressures Calculated for 4100 Hertz Elastic Scattering

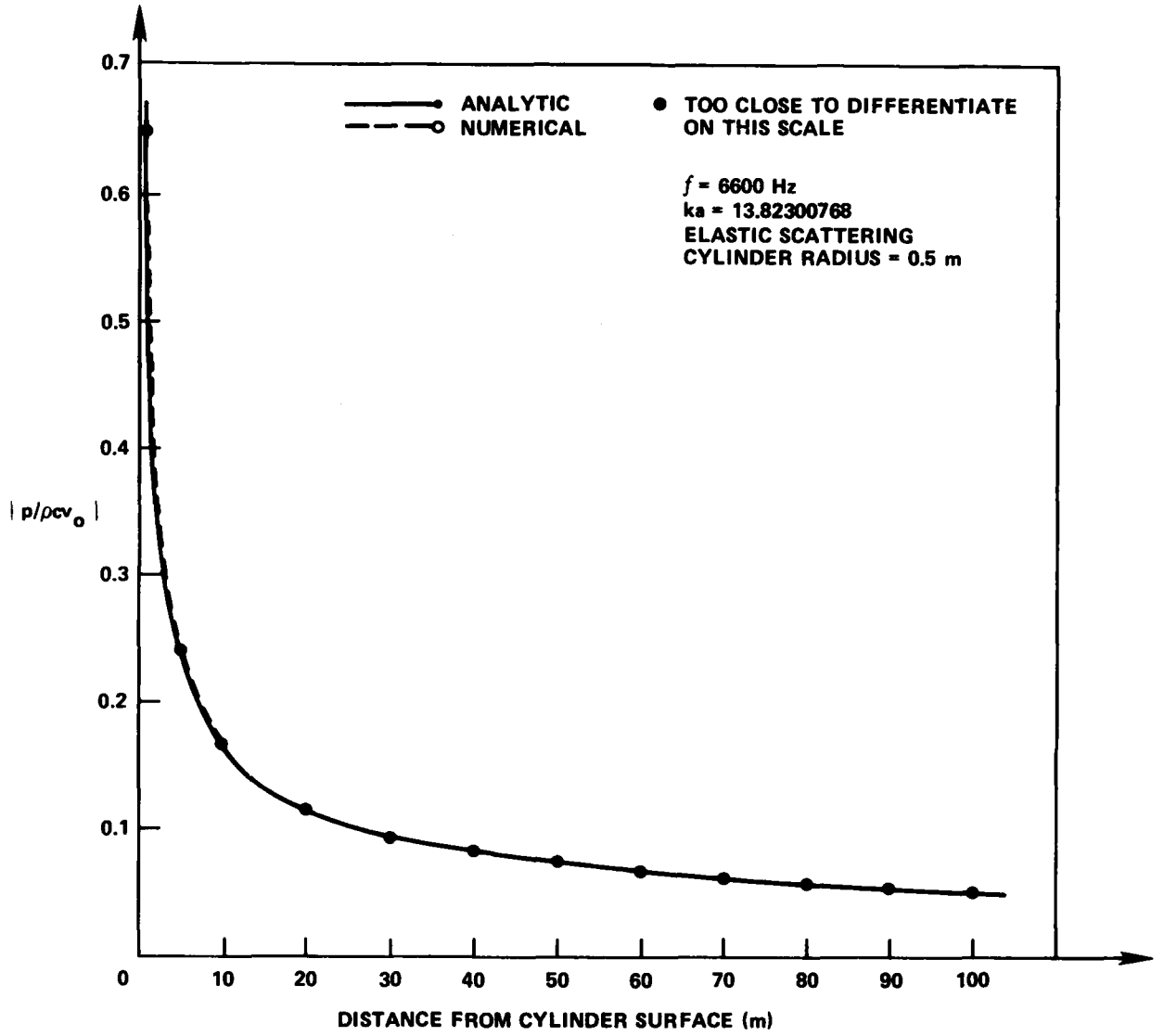

Figure 14 - Field Pressures Calculated for 6600 Hertz Elastic Scattering

and 25 of Reference 1). Similarly, the excellent agreement of the computed field presssure with the analytic results for the 6600 Hz case, see Figure 14, seems to relate to the fact that, despite rather large discrepancies in the input pressures on the shadowed surface of the cylinder, the pressures in the neighborhood of $\theta = 0$ degrees are very good (see Figure 25 of Reference 1).

SUMMARY

A method has been described for calculating the scattered sound pressure field exterior to infinitely long structures of arbitrary cross section when pressure and velocity normal to the cross section boundary are known.

The method is derived by combining the capabilities of two existing computing methods: one, a finite-element approach to fluid-structure interaction problems, and the other, an algorithm for numerical quadrature of the Helmholtz equation which relates exterior field pressures to pressure and normal velocity over a 3-D structural boundary.

Application of the method to the calculation of the field pressures exterior to infinite cylinders for rigid and elastic scattering gave pressures in excellent agreement with analytic results.

The considerable versatility of the finite-element formulation, combined with the equal versatility of the quadrature algorithm, gives a method which is applicable to a wide range of structural configurations and geometries. In view of this, the method offers a useful tool for obtaining comparison data which may serve as a basis for the testing and refining of analytic approaches, as well as a means for obtaining solutions for cases not presently within the range of analytic approaches.

Extension of the method to 3-D, apart from requiring more computation, is trivial, since both the finite-element and quadrature formulations are inherently 3-D.

ACKNOWLEDGMENTS

The author wishes to express thanks to: Mr. Myles Hurwitz for several very helpful discussions during this investigation; Dr. George Chertock for suggesting some numerical experiments which greatly aided the identification of

certain key relationships between the finite element and quadrature formulations; and Dr. Gordon Everstine for reading the manuscript and offering a number of suggestions for its improvement.

REFERENCES

1. Henderson, F.M., "Computation of Steady-State Scattered Sound from Submerged Infinite Cylinders by a Structural Analog Method," DTNSRDC Report 82/012 (Feb 1982).

2. Everstine, G.C., "Structural-Acoustic Finite Element Analysis, with Application to Scattering," Proceedings of the 6th Invitational Symposium on the Unification of Finite Elements, Finite Differences, and Calculus of Variations edited by H. Kardestuncer, University of Connecticut, pp. 101-122, (May 1982).

3. Everstine, G.C., "A Symmetric Potential Formulation for Fluid-Structure Interaction," Journal of Sound and Vibration, 79(1), pp. 157-160 (8 Nov 1981).

4. Henderson, F.M., "A Guide to Use of the XWAVE Program: Part I - Radiated Pressures from Vibrating Structures," DTNSRDC Report 77-0041 (Jul 1977).

5. Henderson, F.M., "A Guide to Use of the XWAVE Program: Part II - Scattering of Sound Waves from Rigid Structural Surfaces," DTNSRDC Report 78/019 (Feb 1978).

6. Chertock, G., "Integral Equation Methods in Sound Radiation and Scattering from Arbitrary Surfaces," DTNSRDC Report 3538 (Jun 1971).

7. Junger, M.C. and D. Feit, "Sound, Structures, and Their Interaction," The MIT Press, Cambridge, Massachusetts (1972).

8. Davis, J.P. and P. Rabinowitz, "Numerical Integration," Blaisdell Publishing Co., Waltham, Massachusetts (1967).

INITIAL DISTRIBUTION

Copies		
6	ONR	
	1	ONR 411
	1	ONR 411MA
	1	ONR 432
	1	ONR 437
	1	ONR 439/N. Basdekas
	1	ONR 474
1	DNL	
5	NRL	
	1	246/R. Perlut
	1	2310/R. Shimkus
	1	5840/R. Skop
	1	7732/L. Turner
	1	5836/W. Webbon
2	USNA	
	1	Dept. Math
	1	Tech Lib
3	NAVMAT	
	1	MAT 071
	1	MAT 0714
	1	MAT 064
2	NADC	
	1	501/J. Heap
	1	Tech Lib
1	NATC/Patuxent	
	1	Don Louieos
3	NAVPGSCOL/Lib	
	1	G. Cantin
	1	A. Shoenstadt
	1	Tech Lib
1	NAVWARCOL	
2	NCSC	
	1	751/P. Bishop
	1	Tech Lib
2	NOSC/San Diego	
	1	7132/L. McLeary
	1	Tech Lib

Copies		
1	NPRDC	
	1	P311/D. Rahilly
3	NSWC/White Oak	
	1	K22/R.J. Edwards
	1	E22/E. Peizer
	1	Tech Lib
2	NSWC/Dahlgren	
	1	K21/C. Blackman
	1	Tech Lib
2	NUSC/New London	
	1	44/A. Carlson
	1	Tech Lib
2	NUSC/Newport	
	1	3701/C. Curtis
	1	Tech Lib
2	NWC	
	1	32H2/J. Serpanos
	1	Tech Lib
1	NAVAIR	
	1	1154/G. Hand
11	NAVSEA	
	1	SEA 03A
	1	SEA 03R11/J. Sejd
	1	SEA 55Y
	1	SEA 32113/J. Claffey
	1	SEA 03R2/J. Gagorik
	1	SEA 32323/R. McCarthy
	1	SEA 32133/W. Sandburg
	1	SEA 05H/S. Blazek
	1	SEA 05H/C. Taylor
	1	SEA 05R15/H. Vanderveldt
	1	SEA 03R3/P. Anklowitz
1	NAVSHIPYD BREM/Lib	
1	NAVSHIPYD CHASN/Lib	
1	NAVSHIPYD MARE/Lib	

Copies	
1	NAVSHIPYD NORVA/Lib
1	NAVSHIPYD PEARL/Lib
1	NAVSHIPYD PHILA/Lib
1	NAVSHIPYD PTSMH/Lib
12	DTIC
1	Penn State University/ARL
	1 D. Thompson
1	Goodyear Aerospace
	1 G. McDearmon

CENTER DISTRIBUTION

Copies	Code	Name
1	012.4	R. Stevens
1	11	W.M. Ellsworth
1	1182	Z.G. Wachnick
1	15	W.B. Morgan
1	1542	D.F. Thrasher
1	1568	L. Motter
1	16	H. Chaplin
1	17	W.W. Murray
1	1702	J. Corrado
1	172	M.A. Krenzke
1	1720.2	K. Hom
1	1720.3	R.F. Jones
1	1720.6	R.D. Rockwell
1	1730	A.B. Stavovy
1	1730.5	J.C. Adamchak
2	1750.2	B. Whang
		P. Roth
1	18	G.H. Gleissner
1	1802.1	H.J. Lugt
1	1805	E.H. Cuthill
2	1809.3	D. Harris
1	182	A. Camara
1	1824	S. Berkowitz
1	184	J.W. Schot
1	1843	H.J. Haussling
1	1844	S.K. Dhir
5	1844	G.C. Everstine
1	1844	F.M. Henderson
1	1844	M.M. Hurwitz
1	185	T. Corin
1	187	M. Zubkoff
1	189	G. Gray
1	1892.1	J. Strickland
1	19	M.M. Sevik
1	1901	M. Strasberg
1	1902	G. Maidanik
1	1903	G. Chertock
1	1905.2	W. Reader
1	196	D. Feit
3	1962	A.K. Kukk
		T. Eisler
		A. Zaloumis
2	1965	M. Rumerman
		Y.N. Liu
1	1966	J. Casper
1	27	W.C. Deitz
1	272.1	H.N. Urbach
1	2723	P. Hatchard
1	2732	J.W. Dickey
2	274	L.J. Argiro
		Y.F. Wang
1	28	J.R. Belt
1	2822	W. Palko
2	2832	J. Dray
		T. Daugherty
1	29	F.H. Kendall, Jr.
10	5211.1	Reports Distribution
1	522.1	Unclass Lib (C) (1 M)
1	522.2	Unclass Lib (A)
1	93	L. Marsh

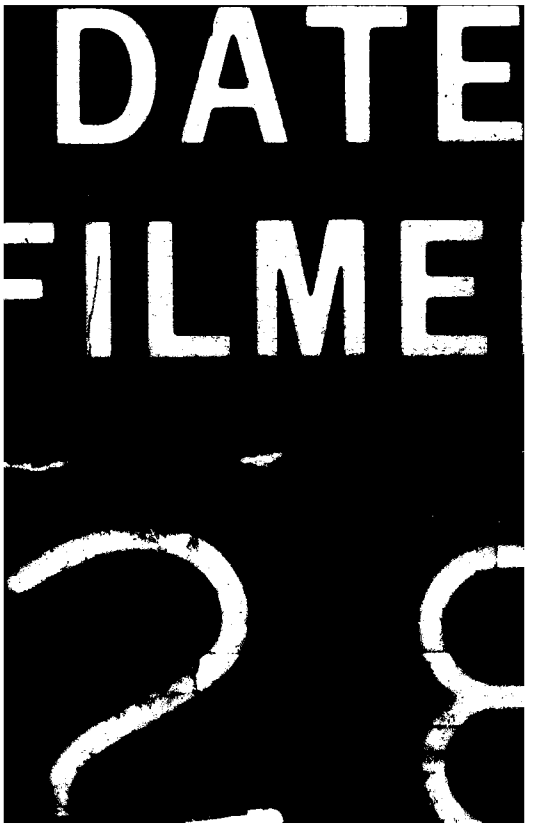
DATE
FILME